Human Aspects of Advanced Manufacturing, Vol. 66, 2022, 40–48
https://doi.org/10.54941/ahfe1002686

Functionalized Multilayer Structures for Burns Treatment

Emilia Visileanu[1], Alexandra Gabriela Ene[1], Alina Vladu[1], Stelian Sergiu Maier[2], and Diana Popescu[3]

[1]The National Research and Developement Institute for Textile and Leather, Bucharest, 030508, Romania
[2]Sanimed International Impex SRL Calugareni, 087040, Romania
[3]The National Research and Development Institute Medico-Military "Cantacuzino" Bucharest , 050096, Romania

ABSTRACT

Complex composites matrix for hemostasis and connective tissue regeneration were developed. The three-layered structure consists of outer layer I which plays the role of carrier, insulator and protector of the underlying layers, being elastic, resistant and sub microporous (to block the physical access of microorganisms to the lesion), layer II – has the purpose of managing the liquid compositions in the lesion area, macro-porous and compressible, with open pores and high tortuosity and layer III - impermeable substrate - non-adherent, biologically inert and microporous. The statistical indicators of the defining variables for each variant of textile structures (intended for layers I and III) are calculated, the histograms, the box plot graphs and the interactive spatial graphs, in the form of band type graphs are drawn. Biocompatibility assessment of textile supports for layers I and III were performed by MTT viability test and the LDH cell integrity test. The in vitro study for testing the biocompatibility of the functionalized multilayer matrix showed that they are biocompatible because the phenomenon of cell adhesion was present, regardless of the cell line used. In vivo testing according to ISO 10993-6 used the model of thermal burn injury on white rats (Wistar albino). The treated rats showed a rate of rapid healing and at 7 days of treatment the closure of the wound was observed between 40%–60%, with areas of tissue regeneration. Inhibition of the invasion of exogenous microorganisms has been noted.

Keywords: Composite, Matrix, Regeneration, Tissue, Burn, Biocompatibility

INTRODUCTION

Despite the current topical treatment methods designed to eradicate the bacterial load present in the burn wound, sepsis remains the leading cause of death in burn treatment units worldwide (Pengju et al. 2021). Advances in resuscitation, surgical management, infection control, hypermetabolic response control, and rehabilitation have resulted in significant improvements in burn mortality and morbidity over the past 60 years (Vivó et al. 2016), (Toussaint, et al. 2014). Burns are classified according to their depth and severity in grades I, II, III and IV (Rowan et al. 2014). Severely burned skin ceases to fulfill its natural role of protection and barrier and promotes

a dramatic increase in water loss and can become a gateway for bacterial invasion. Many physiological properties of the burned area predispose to infection and inhibit traditional treatment with systemic antibiotics (Shpichka et al. 2019), (Alharbi, 2012). The solution developed to solve these problems is to create a three-layered medical device, with compo-site characteristics, usable for summary medical interventions on lesions with an optimistic prognosis at first assessment: superficial burns with thermal origin (flame and melts) occurred on anatomical regions protected by clothing (except face and eyes). The device provides antimicrobial and analgesic effects, as well as fluid management in the injured region, through local transfer processes (sorption/desorption in porous media). The general para-medical effects stated, as well as the effects specific to each variant (hemostasis/firm adhesion/compression) and respectively application / removal without affecting the tissues, are ensured based on the alternation of three layers, which form the generic structure of the medical device.

MATERIALS AND METHODS

The three-layered structures consist of three layers with well-defined roles: i) The interfacing layer with the lesion: non-adherent, biologically inert and microporous. (ii) The middle layer: intended for the management of liquid compositions in the lesion area, macro-porous and compressible, with open pores with high tortuosity. (iii) Outer layer: carrier, insulator and protector of the underlying layers, being elastic, resistant and sub-microporous (to block the physical access of microorganisms to the lesion). The interfacing layer and the outer layer were made by classical technologies (weaving and interweaving) and the middle layer by technologies in the field of (bio) macromolecular compounds processing.

Layer 1

The woven textile support (Layer 1) was made of yarn: 100% cotton 20x2 / 50/2 (Tex/Nm) in warp and 80% cotton + 20% ZnO-14.8x2 / 68/2 (Tex/Nm) in weft. The techniques provided by descriptive statistics were used to characterize the selected raw materials. The characteristics considered for those yarn variants used for layer I were: length density, torsion/twist, hygroscopicity, breaking load, elongation at break. The attributes of the 5 variables obtained from the experiments were defined in Data Editor and Variable View specific to a specialized program. For all the characteristics of the experienced variants, the Q-Q Plot graphs were used, which allow both the detection of the aberrant values and the verification of the normality of the distributions. For the theoretical distribution (in this case - the normal distribution) the quantile values are represented by a line that passes through the origin and has slope 1; if the points Q-Q outline a line that overlaps with the line that represents the normal distribution, then it can be stated that the distribution of the tested variable is normal (see Fig. 1). Estimation method used: Van der Waerden.

For the woven structure, the technological flow, the assembly and adjustment parameters, the programming scheme were established (see Fig. 2). To

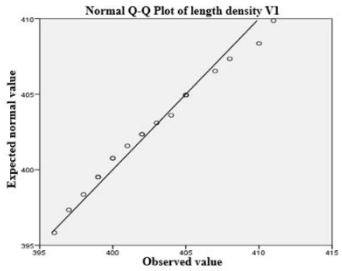

Figure 1: Q-Q Plot for length density variable a) V1.

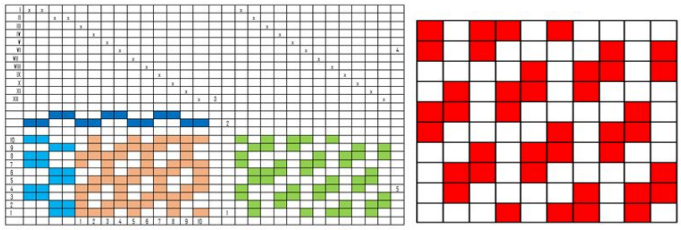

Figure 2: Compound atlas link programming scheme.

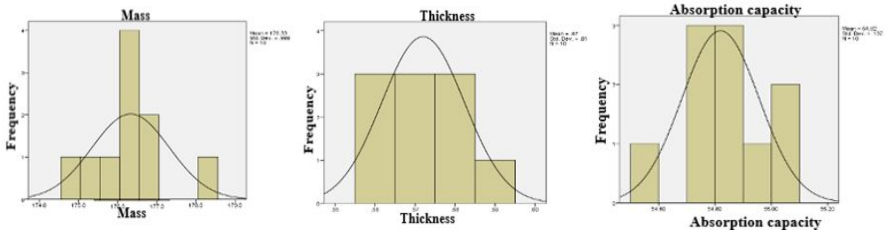

Figure 3: Histograms of variables - V1: a) mass; b) thickness; c) static absorption capacity.

characterize the planar structure used to create the first layer of the matrix, the methods specific to descriptive statistics were used. Thus, with the help of a specialized program it was possible to rigorously describe the resulting distributions as a result of the characterization of textile structures. They were calculated for each of the 3 variables considered defining for a woven structure: mass, thickness and absorption capacity, the following fundamental statistical indicators: mean, dispersion and standard deviation, median and quartiles, eccentricity (skewness) and vaulting (kurtosis) for asymmetry and highlighting the cases in which interventions should be performed. Histograms (see Fig. 3) and boxplot graphs (see Fig. 4) of the variables mass, thickness and static absorption capacity were plotted.

Interactive spatial graphs were also drawn in the form of band-type graphs (Fig. 5).

Layer 3

The non-woven one from: 50% chitosan / 80% Tencel was used for layer III. For the flat structure made by the non-woven technology (layer III) the mass,

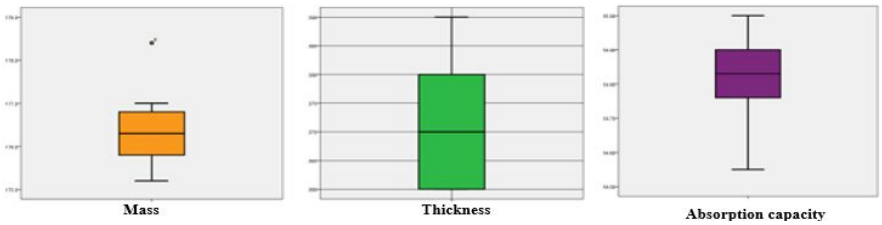

Figure 4: Boxplot graphics for V1: a) mass, b) thickness, c) static absorption capacity.

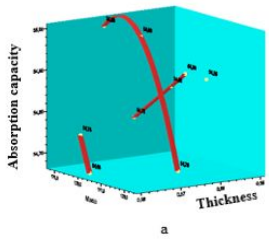

Figure 5: Band graphs for V1.

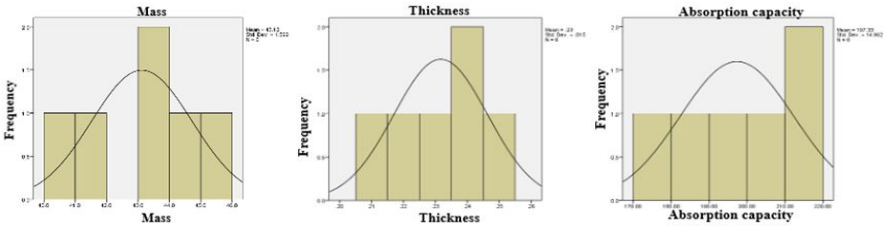

Figure 6: Histograms of variables V3: a) mass, b) thickness, c) absorption capacity.

thickness, absorption capacity, tearing force (longitudinal and traversal), breaking force (transversal and longitudinal) elongation at max (longitudinal and transversal) were determined. The following fundamental statistical indicators: were calculated for each of the 9 variables considered defining for a nonwoven structure: mean, dispersion and standard deviation, median and quartiles, eccentricity (skewness) and vault (kurtosis) for asymmetry and the cases in which interventions should be per-formed were highlighted. Histograms (see Fig. 6) and boxplot graphs (see Fig. 7) of the variables mass, thickness and static absorption capacity were plotted. Interactive spatial graphs were also drawn in the form of band-type graphs (see Fig. 8).

Layer 2

The second (middle) layer of the matrix with medical device characteristics has the role of being loaded with an aqueous composition composed of pharmacologically-active species, of retaining them by inhibition and of releasing them in a time-dependent manner, when used. Such a role can be played by medium and highly crosslinked polymeric hydrogels, capable of post-hydration in the presence of an excess of biological fluids. One of the polymeric systems that ensure simultaneously a good biocompatibility and

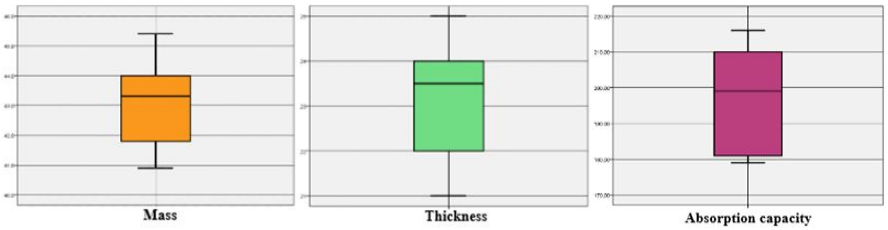

Figure 7: Boxplot graphics for V3: a) mass, b) thickness, c) static absorption capacity.

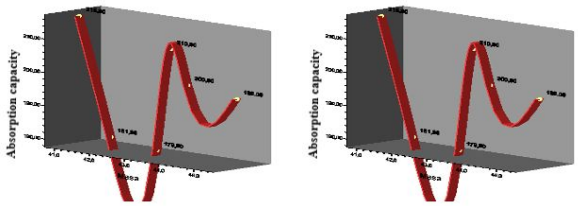

Figure 8: Interactive spatial graphs.

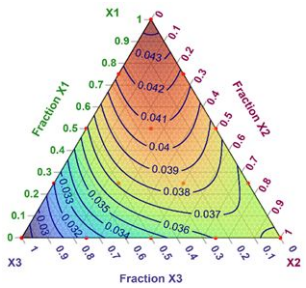

Figure 9: Ternary diagram of relative density dependence.

a high hydration capacity (systems capable of forming hydrogels) is represented by polyurethane copolymers, possibly belonging to the subclass of block-copolymers. Fig. 9 shows, in the format of a ternary diagram described by constant level curves, the variation of the values of the apparent density of the hydrogels prepared according to the experimental matrix, as a function on the composition of the polyol mixture. The organoleptic observation of the characteristics of the obtained hydrogels suggests that the samples with a density between 0.035-0.04 g/cm^3 allow the optimization of the recipes of polyol mixtures. Comparisons were made between the effect of compositional variations around some points of the ternary diagram that simultaneously meet two conditions derived from practical reasons: (i) placement in regions close to the quasi-optimal value in question, and (ii) working with mixing ratios easy to make between polyol components (see Fig. 10).

The poly-PG component, with the role of chain extender, is the one that ensures the "background" of the property value. Also, for all compositions, poly-CAT, is the crosslinking agent, has the most influence on the variations of the measured property. The PG component, propylene glycol, with the role of regulating the compactness of the hydrogel, acts paradoxically, decreasing the relative density and not increasing it, probably because it can

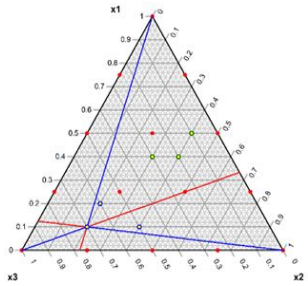

Figure 10: Analysis of the stability of the measured values.

act as an agent that stops the polymerization. Only in the compositions in which it becomes dominant, the PG component acts in the sense of increasing the apparent density and, most likely, the compactness of the hydrogel. Figure 10 compares the evolutions around the points placed in a region of the diagram in which the apparent density of hydrogels has a higher value (0.040 g/cm^3), these being firmer, thinner and less porous. Although the effects of compositional variations are similar to those that provide lower bulk densities (0.035 g/cm^3), the amplitude of the effects differs. The variation of the PG component content (X3) becomes dominant in relation to the variation of the other two components of the polyol mixture. Thus, the effect of stopping the polymerization, induced by propylene glycol, is more pronounced. The three-layered structure was achieved by flanking the hydrogel with the textile materials designed for layers I and III. An important component of the human systems integration plan should be a verification and validation process that provides a clear way to evaluate the success of human systems integration. The human systems integration team should develop a test plan that can easily be incorporated into the systems engineering test plan. The effectiveness and performance of the human in the system needs to be validated as part of the overall system. It may seem more attractive to have stand-alone testing for human systems integration to show how the user interacts with controls or displays, how the user performs on a specific task. This methodology can address the performance of the human operator or maintainer with respect to the overall system. The most important thing is to develop a close relationship between human systems integration and systems engineering.

Biocompatibility- In Vitro Study

The multilayer biocompatibility study was performed by in vitro and in vivo tests. Two cell lines were used to perform the multilayer matrix cytotoxicity / cell viability test: Rat dermal fibroblasts and Rat keratinocytes using the commercial MTT Assay Kit (Sigma). Cell proliferation was also quantified by the MTT test. The adhesion efficiency of fibroblast and keratinocyte cells was established and the results were compared with untreated control (see Fig. 11).

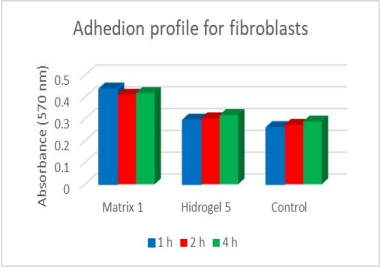

Figure 11: Absorbance values.

Biocompatibility- In Vivo Study

To study the repair processes in the presence of the functionalized multilayer matrix, we used the thermal burn injury model on white rats (Wistar albino). After burn induction and bandages application, the animals were monitored daily for various clinical signs, weight loss, and wound closure. The wounds were examined at 0, 3, 7 and 10 days after the burn injury induction and the wound areas were measured. The wound healing rate (WHR) was defined using the following equation (1):

$$WHR\ (\%) \ = \ (AO \ - \ An)/AO\ x\ 100\%[5] \qquad (1)$$

where An is the area of the wound on a given day (3, 7, 10 days) after causing the burn injury, and AO is the initial area of the wound.

The dressings were replaced 3, 7 and 10 days after the burn (or if necessary) and at the same time, 2 rats from each batch (including the control batch) were slaughtered.

RESULTS AND DISCUSSION

Characterization of Layers

The prediction calculated for the 2 yarn variants from which the woven textile structures for Layer I, were made does not fully correspond with reality but can give important information regarding the design of woven structures, such as:

- the possibility of combining yarns, depending on the length density;
- the length of the binding segments and implicitly the size of the ratios: small binding segments 1 or 2, or large ones of maximum 5 (in order not to compromise the stability of the fabric); reports in the warp of 8 - 18, reports in weft in the interval 10 - 14;
- possible densities to be achieved in order to obtain an optimal thickness in the whole matrix: Du = 180 - 250 yarns/10 cm, Db = 200 - 350 yarns/10 cm.

The variables “mass”, “thickness” and “absorption capacity” of the woven structures (layer 1) do not show great variability of the results.

The analysis of statistical data for the V3 textile structure shows the following aspects:

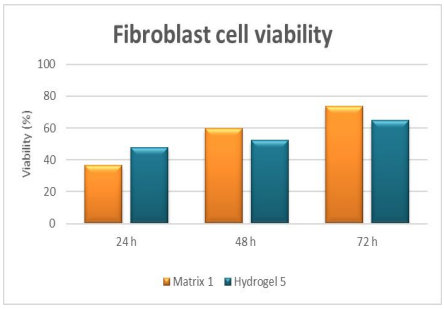

Figure 12: Cellular viability.

Figure 13: Wound evolution.

- 25% of the values obtained for the mass are above the value of 44.35 g/sqm, 25% being in the range [43.3; 44.35] and 25% below 41.6 g/sqm;
- 25% of the values obtained for thickness are below the value of 0.22 mm and 25% above the value of 0.24 mm;
- 25% of the values of the absorption capacity are below 180%, 50% are in the range [1808; 212] and 25% are above the upper limit of the range;
- skewness indicators have negative values for all variables, below -1.96, so the distribution function is normal, the curves moving to the left.

Biocompatibility Testing

It has been observed that the phenomenon of cell adhesion is present regardless of the cell line used. At one hour, the matrix showed significant cell adhesion compared to pure hydrogel and control of untreated lamellae (much less adherent). At 2 hours, an increase in absorbance values is observed, which translates into an increase in the number of adherent cells. At 4 hours after seeding, the number of cells attached to the substrate decreased slightly. Fibroblast and keratinocyte proliferation was analyzed at 24, 48, and 72 hours of substrate-cell interaction (see Fig. 12).

The growing number of the two cell types used for viability testing shows that proliferation occurs on the experimental matrix.

Wound Healing Rate

The wound healing rate for each wound was assessed by determining (measuring) the unhealed area of the wound as a function of time. The treated rats

showed a rate of rapid healing and at 7 days of treatment, the closure of the wound was observed approximately 60% (see Fig. 13) with areas of tissue regeneration.

An inhibition of the invasion of exogenous microorganisms was also observed, probably due to the inherent antimicrobial property of the demonstration models used. The results of the wound healing studies suggested that all 4 test models tested could be used as potential dressings with regenerative properties for burn wounds.

CONCLUSION

A structure for the treatment of burns was designed and made of 3 layers: layer I - 100% cotton 20x2 / 50/2 (Tex / Nm) in warp and 80% cotton + 20% ZnO-14.8x2 / 68/2 (Tex / Nm)in weft, layer III - nonwoven from: 50% chitose / 80% Tencel and the binding layer from hydrogel. The multilayer structure was made by flanking the hydrogel with the textile structures that form layer I and layer III. The biocompatibility of the multilayer structure achieved by in vitro studies showed that the phenomenon of cell adhesion is present regardless of the cell line used. The increasing number of fibroblasts and keratinocytes showed the production of matrix proliferation. The biocompatibility of the multilayer structure performed by in vivo studies showed a rate of rapid healing and at 7 days of treatment, it was observed the closure of the wound was approximately 60% with areas of tissue regeneration.

ACKNOWLEDGMENT

This research is carried out within the project: Innovative medical device for emer-gency and operational medicine “CELLMATRIX”, PN-III-P2-2.1-PED-2019.

REFERENCES

Alharbi Z., Piatkowski A., Dembinski R., Reckort S., Grieb G., Kauczok J., Pallua N (2012).: Treatment of burns in the first 24 hours: simple and practical guide by answering 10 ques-tions in a step-by-step form,World Journal of Emergency Surgery vol. 7, Article number: 13.

Pengju Z., Bingwen Z., Yih-Cherng L., Canhua H.: Burns & Trauma, (2021) Volume 9, tkaa047, https://doi.org/10.1093/burnst/tkaa047.

Rowan M. P., Cancio L.C., Elster E. A., Burmeister D. M., Rose L. F., Natesan S., Chan R. K., Christy R. J., Chung K. K. (2015): Burn wound healing and treatment: review and ad-vancements, Crit Care. 19: 243.Published online 2015 Jun 12. doi: 10.1186/s13054-015-0961-2.

Shpichka A., Butnaru D., Bezrukov E.A., Sukhanov R.B., Atala A., Burdukovskii V., Zhang Y., Timashev P. (2019): Skin tissue regeneration for burn injury, Stem Cell Research & Therapy volume 10, Article number: 94.

Toussaint J., Singer A.J. (2014): The evaluation and management of thermal injuries: Clinical and experimental emergency medicine. [PubMed PMID: 27752547].

Vivó C, Galeiras R, del Caz M.D. (2016): Initial evaluation and management of the critical burn pa-tient. Med Intensiva. 40(1):49-59 [PubMed].